BJR

Received: 30 April 2016 | Revised: 4 August 2016 | Accepted: 12 September 2016

http://dx.doi.org/10.1259/bjr.20160379

Cite this article as:
Bo X-W, Xu H-X, Wang D, Guo L-H, Sun L-P, Li X-L, et al. Fusion imaging of contrast-enhanced ultrasound and contrast-enhanced CT or MRI before radiofrequency ablation for liver cancers. *Br J Radiol* 2016; **89**: 20160379.

FULL PAPER

Fusion imaging of contrast-enhanced ultrasound and contrast-enhanced CT or MRI before radiofrequency ablation for liver cancers

XIAO-WAN BO, MD, HUI-XIONG XU, MD, PhD, DAN WANG, MD, LE-HANG GUO, MD, LI-PING SUN, MD, XIAO-LONG LI, MD, CHONG-KE ZHAO, MD, YA-PING HE, MD, BO-JI LIU, MD, DAN-DAN LI, MD and KUN ZHANG, PhD

Department of Medical Ultrasound, Shanghai Tenth People's Hospital, Ultrasound Research and Education Institute, Tongji University School of Medicine, Shanghai, China

Address correspondence to: Prof. Hui-Xiong Xu
E-mail: *xuhuixiong@126.com*

Objective: To investigate the usefulness of fusion imaging of contrast-enhanced ultrasound (CEUS) and CECT/CEMRI before percutaneous ultrasound-guided radiofrequency ablation (RFA) for liver cancers.
Methods: 45 consecutive patients with 70 liver lesions were included between March 2013 and October 2015, and all the lesions were identified on CEMRI/CECT prior to inclusion in the study. Planning ultrasound for percutaneous RFA was performed using conventional ultrasound, ultrasound-CECT/CEMRI and CEUS and CECT/CEMRI fusion imaging during the same session. The numbers of the conspicuous lesions on ultrasound and fusion imaging were recorded. RFA was performed according to the results of fusion imaging. Complete response (CR) rate was calculated and the complications were recorded.
Results: On conventional ultrasound, 25 (35.7%) of the 70 lesions were conspicuous, whereas 45 (64.3%) were inconspicuous. Ultrasound-CECT/CEMRI fusion imaging detected additional 24 lesions thus increased the number of the conspicuous lesions to 49 (70.0%) (70.0% *vs* 35.7%; $p < 0.001$ in comparison with conventional ultrasound). With the use of CEUS and CECT/CEMRI fusion imaging, the number of the conspicuous lesions further increased to 67 (95.7%, 67/70) (95.7% *vs* 70.0%, 95.7% *vs* 35.7%; both $p < 0.001$ in comparison with ultrasound and ultrasound-CECT/CEMRI fusion imaging, respectively). With the assistance of CEUS and CECT/CEMRI fusion imaging, the confidence level of the operator for performing RFA improved significantly with regard to visualization of the target lesions ($p = 0.001$). The CR rate for RFA was 97.0% (64/66) in accordance to the CECT/CEMRI results 1 month later. No procedure-related deaths and major complications occurred during and after RFA.
Conclusion: Fusion of CEUS and CECT/CEMRI improves the visualization of those inconspicuous lesions on conventional ultrasound. It also facilitates improvement in the RFA operators' confidence and CR of RFA.
Advances in knowledge: CEUS and CECT/CEMRI fusion imaging is better than both conventional ultrasound and ultrasound-CECT/CEMRI fusion imaging for lesion visualization and improves the operator confidence, thus it should be recommended to be used as a routine in ultrasound-guided percutaneous RFA procedures for liver cancer.

INTRODUCTION

Hepatocellular carcinoma (HCC) is the sixth most common cancer and the third leading cause of cancer-related death in the world.[1–3] Percutaneous radiofrequency ablation (RFA) and microwave ablation are the most widely used minimal invasive modalities for the treatment of liver cancer, especially for small tumours.[4–8] RFA is usually guided by conventional ultrasound or CT.[9] Ultrasound-guided RFA is more extensively used because of the virtues of conventional ultrasound such as real-time scanning, convenience, wide availability and no radiation. However, because of the relatively low spatial resolution and penetration, coarse background of associated liver cirrhosis, interference of bowel gas and limited acoustic window, some lesions show poor conspicuity on conventional ultrasound.

In comparison with non-enhanced conventional ultrasound, contrast-enhanced imaging such as contrast-enhanced ultrasound (CEUS), contrast-enhanced CT (CECT) or contrast-enhanced MRI (CEMRI) improves the signal-to-noise ratio after administration of contrast media and facilitates detection of focal liver lesions with or without cirrhotic liver background.[10–12] Among them, CEUS has been proven to have similar diagnostic performance for characterization of liver cancer compared with

CECT/CEMRI.[13–16] In addition, CEUS is convenient and can be performed instantly after conventional ultrasound, which is relevant in clinical practice since most RFA procedures are performed under ultrasound guidance so that CEUS and conventional ultrasound can be carried out in the same setting for RFA guidance and treatment planning. Nevertheless, CEUS alone can not avoid all the shortcomings of conventional ultrasound such as interference of bowel gas and limited acoustic window. The limited arterial phase (usually <10–15 s) of CEUS also restricted its application for guidance since the RFA electrode placement is hardly achievable in such a short period. As a consequence, sometimes, repeat administration of contrast agent is necessary. On the other hand, CECT/CEMRI has higher spatial resolution and the panorama view facilitates the visualization of the spatial relationship between the target lesion and adjacent critical structures (*e.g.* stomach, gallbladder, gut and so on), which improves the confidence level of the operator and reduces unwanted damage to these structures. However, CECT/CEMRI is expensive and not widely available. CECT also has radiation, and the guidance by CECT/CEMRI usually costs a lot of time.

Fusion imaging combines the advantages of ultrasound and CT/MRI, whereas avoids their disadvantages, which is a technique that can display ultrasound and CT/MRI images simultaneously on the same setting.[17–20] It is often achieved by using a magnetic navigation system which allows coordination of two different imaging modes and allows their display on the same screen. With the help of the position-sensing unit, the ultrasound image moves following the CT/MRI image. After the two images match well, the target lesion on ultrasound image can be located according to the CT/MRI image. Previous studies[21–23] reported that ultrasound-CECT/CEMRI image fusion technique could detect more tumours than conventional ultrasound (53.3–98% *vs* 38.8–66%), and it facilitates RFA for liver tumours with poor conspicuity on conventional ultrasound.[17,24–26] However, even with the help of ultrasound-CECT/CEMRI fusion, some lesions still show suboptimal conspicuity on the images of conventional ultrasound, and CEUS is often necessary to confirm the exact location and configuration of the target lesion. The fusion of CEUS and CECT/CEMRI before RFA might further enhance the lesion conspicuity and operator confidence in that the inconspicuous lesions would show arterial hyperenhancement in both modalities, thus the lesions are easily detectable. To confirm the hypothesis, the study was aimed to investigate the usefulness of CEUS and CECT/CEMRI fusion imaging before RFA for liver cancers.

METHODS AND MATERIALS

Patients

From March 2013 to October 2015, 46 consecutive patients with 73 liver cancers were planned for percutaneous ultrasound-guided RFA in the Shanghai Tenth People's hospital. The approval from the ethics committee of the university hospital was obtained, and all patients had signed informed consent before the procedures. The rationale for the study was that RFA was carried out under ultrasound guidance, and all the lesions should be confirmed on CECT/CEMRI before RFA. In addition, fusion of ultrasound-CECT/CEMRI and CEUS and CECT/CEMRI was routinely used to reconfirm the lesion before ultrasound-guided RFA. The interval between ultrasound and CECT/CEMRI procedures was within a week. The inclusion criteria were as follows: (1) all the patients underwent CECT/CEMRI before RFA and all the lesions were visualized clearly on CECT/CEMRI; (2) all the patients underwent ultrasound/CEUS and CECT/CEMRI fusion imaging; (3) no more than five lesions in each patient; (4) the maximal diameter of each lesion was no more than 5 cm; and (5) with more than 3 months' follow-up after RFA. Of the 46 patients who had undergone fusion imaging, 45 consecutive patients (35 males, 10 females; mean age, 56.42 ± 9.44 years; age range, 35–73 years) with 70 lesions were finally included in this study except for 1 patient with 3 lesions who was lost during follow-up. Table 1 shows the patients' clinical characteristics. The diagnosis of HCC was in accordance with the American Association for the Study of Liver Diseases guideline.[27] HCC was diagnosed with arterial hypervascularity and venous or delayed phase washout on 4-phase multidetector CT or dynamic contrast-enhanced MRI or pathological results after percutaneous biopsy. The diagnosis of metastatic liver cancer or intrahepatic cholangiocellular carcinomas (ICCs) was confirmed by percutaneous biopsy, or pathological results of original tumours in combination with typical CT/MRI findings and serum biomarkers. Finally, there were 32 patients with HCCs (14 primary HCC lesions; 31 recurrent HCC lesions), 2 patients with ICCs (7 recurrent ICC lesions) and 11 patients with metastatic liver cancers (7 from colon, 1 from rectum, 1 from breast, 1 from stomach and 1 from nasopharynx). In the 45 patients, 26 patients had 1 lesion, 14 patients had 2 lesions, 4 patients had 3 lesions and 1 patient had 4 lesions. Of the 70

Table 1. Baseline clinical characteristics of the patients

Characteristics	Values
Age (years)[a]	56.4 ± 9.4 (35–73)
Sex	
Male/female	35/10
Liver function	
Child–Pugh classification A/B/C	45/0/0
Lesion nature	
HCC/ICC/MLC	45/7/18
Previous treatment	
None/TACE or RFA	63/7
Tumour number	
One/two/three/four	26/14/4/1
Tumour segment	
S1/S2/S3/S4/S5/S6/S7/S8	0/2/7/10/12/23/7/9
Tumour size (cm)	
≤2.0/2.1–5.0 cm[a]	1.4 ± 0.3/2.8 ± 0.8

HCC, hepatocellular carcinoma; ICC, intrahepatic cholangiocarcinoma; MLC, metastatic liver cancer; RFA, radiofrequency ablation; TACE, transcatheter arterial chemoembolization.
[a]Mean ± standard deviation. Numbers in parentheses are ranges.

lesions, 28 were ≤2.0 cm and 42 ranged from 2.1 to 5.0 cm. The mean maximal diameter of these lesions was 2.0 ± 0.9 cm (range, 0.8–5.0 cm).

Equipment and techniques

Ultrasound examination was performed using a LOGIQ E9 scanner (GE Healthcare, Milwaukee, WI) with a 1–5 MHz curved-array transducer. The image fusion system was composed of the ultrasound scanner with dedicated built-in hardware and software. The SonoVue® (Bracco, Milan, Italy) was used as the ultrasound contrast agent. A dose of 1.5 ml was usually used for administration from the antecubital vein and then followed with a flush of 5 ml of normal saline. The mechanic index was controlled to be <0.2 when the contrast-specific mode was applied so that the microbubbles in the circulation would not be disrupted. The enhancement pattern of the lesions on arterial (10–30 s after contrast administration), portal (31–120 s) and late phases (121–360 s) was recorded and reviewed later.

A 3.0-T whole-body MR imager (Verio 3.0 T; Siemens Medical Systems, Berlin, Germany) was used to perform MRI. A dynamic breath-hold gadolinium-enhanced, three-dimensional gradient echo T_1 weighted pulse sequence was performed with imaging in the arterial, portal venous and delayed phases. The CT images were obtained with a spiral scanner (LightSpeed™ VCT, multidetector CT; GE Medical Systems, Milwaukee, WI) before and after injection of intravenous non-ionic contrast with inspiration breath-hold in the hepatic arterial (35 s after injection), portal venous (65 s) and late phases (125 s) of enhancement. A total of 100 ml of non-ionic contrast material containing 300 mg I ml^{-1} was injected with an automatic power injector at a rate of 2–3 ml s^{-1}.

A bipolar RFA system (CelonLabPower, olympus-celon Teltow, Germany) was used in all ablation procedures. This system does not need grounding pads because the electric current develops a circuit in the front end of the electrode needle. The T_{30} (the conducting part of the applicator is 30 mm, including both the insulator and the tip) and T_{40} (the conducting part of the applicator is 40 mm, including both the insulator and the tip) electrode needles were used in the study. The diameter of these electrode needles are 15.5 gauge. The types and numbers of the electrode needles were selected according to the sizes and locations of the lesions. The output energy and power were set according to the needle type used. The ablation procedure would stop automatically when the impedance increased to an extent to prevent carbonization.

Conventional ultrasound and fusion imaging before radiofrequency ablation

Fusion imaging is carried out on the basis of the magnetic navigation system. The magnetic navigation system includes a magnetic field generator and two receivers (*i.e.* position sensors; GE Healthcare). The distance of the magnetic field generator and the position sensors should be <40 cm so that the sensors can receive the signals generated from the magnetic field generator. After the image fusion system was connected with the ultrasound scanner, and the patient lay in the operating bed with supine position, the operator started to scan the patient. Conventional ultrasound was firstly used to observe and locate the target lesion. The lesion and patient characteristics [lesion size, echogenicity, location and depth, relationship to liver capsule and great blood vessels, associated chronic hepatic disease and previous treatment history with RFA or transcatheter arterial chemoembolization (TACE)] were evaluated and were compared between the inconspicuous and conspicuous lesions on conventional ultrasound. When the distance between the lesion and liver capsule was ≤1.0 cm, the lesion was regarded as being in close relationship with the capsule. In addition, when the distance between the lesion and intrahepatic great blood vessels (*e.g.* intrahepatic blood vessel with diameter >0.3 cm, such as intrahepatic portal vein or hepatic vein or hepatic artery) was ≤1.0 cm, the lesion was regarded as being in close relationship with the great blood vessels.

The CECT/CEMRI digital imaging and communications in medicine format data were imported to the ultrasound machine. Then, the ultrasound and CECT/CEMRI images were adjusted to show the same plane on both modalities. For image registration, the sagittal part of the left branch of portal vein image on conventional ultrasound was usually applied to coordinate with the image on CECT/CEMRI. The arterial or portal phase CECT/CEMRI was often selected for fusion with the ultrasound image. The hepatic vein, the intrahepatic cyst or other remarkable reference markers on both conventional ultrasound and CECT/CEMRI were locked and displayed simultaneously to further tune the images. Then, the ultrasound transducer was moved slowly to find the lesion on conventional ultrasound according to CECT/CEMRI. The reference points around the lesions were also further registered simultaneously on conventional ultrasound and CECT/CEMRI. After adjusting the image position on the two modalities through the overlay function, the location of the lesion could finally be confirmed. The patient was asked to keep a uniform and slow respiration so that the observers could coordinate the images accurately. After ultrasound and CECT/CEMRI images matched well, the lesions that were inconspicuous on ultrasound could be located precisely corresponding to CECT/CEMRI imaging. Afterwards, CEUS was applied routinely to confirm the size and location of the lesions. Then, the proper type of electrode needle was selected and fusion-guided RFA was carried out. All the procedures were performed by one operator who had more than 5 years' experience in ultrasound-guided RFA and fusion imaging.

The imaging parameters and the lesion conspicuity, the confidence levels for performing RFA were all evaluated by two operators with consensus and both operators had more than 5 years' experience in ultrasound-guided RFA and fusion imaging. The inconspicuous lesion means the lesion is hazy, indeterminate, concealed or hidden. The confidence level of the operator for performing RFA was evaluated, which was mainly depended on the lesions' conspicuity. The confidence level of the operator for performing RFA was divided into three levels: Level I = no confidence for performing RFA; Level II = confident for performing RFA; and Level III = highly confident for performing RFA. In the current study, the primary end point was lesion conspicuity and the second end point was confidence level of the operator.

Assessment of the ablation zones after radiofrequency ablation and follow-up protocol

1 month after RFA, CECT/CEMRI was used to assess the therapeutic response. No enhancement in the ablation zone and a sufficient safety margin (*i.e.* >5 mm) indicated complete response (CR) after RFA; otherwise, incomplete response was defined. Thereafter, all patients underwent follow-up with CECT/CEMRI or CEUS and laboratory tests, including serum tumour marker tests once every month for the first 3 months and every 3 months later. Local tumour progression (LTP) was defined as any arterial hyperenhancing tumour detected by CECT/CEMRI at the treated area of the ablation lesion in the follow-up period. Distant recurrence was defined as any new intrahepatic and extrahepatic recurrence outside the ablation zone.

Statistical analysis

SPSS® statistical software v.20.0 (IBM Corp., New York, NY; formerly SPSS Inc., Chicago, IL) was used to perform statistical analysis. All continuous data were expressed as mean ± standard deviation if normal distribution was achieved. The comparisons in lesion conspicuity on conventional ultrasound, ultrasound-CECT/CEMRI fusion imaging and CEUS and CECT/CEMRI fusion imaging were analyzed using McNemar test. The comparisons of proportion of the lesion size, echogenicity, location and depth, relationship to the liver capsule and great blood vessels, patients with associated chronic hepatic disease between the inconspicuous lesions and the conspicuous lesions on conventional ultrasound were performed using χ^2 test. The comparison of proportion of the lesions with previous treatment history with RFA or TACE between the inconspicuous lesions

Figure 1. A 43-year-old male with a hepatocellular carcinoma (maximum diameter = 1.7 cm) in Segment VIII of the liver. (a) The lesion (arrows) is inconspicuous on ultrasound-contrast-enhanced MRI (CEMRI) fusion imaging. (b) The lesion (arrows) shows homogeneous hyperenhancement and is conspicuous during the arterial phase of contrast-enhanced ultrasound (CEUS). (c) Transarterial chemoembolization (TACE) is carried out thereafter and the lesion (arrows) is conspicuous after TACE on ultrasound-CEMRI fusion imaging. (d) The lesion (arrows) shows peripheral hyperenhancement and central non-enhancement during the arterial phase of CEUS after TACE. (e) The lesion (arrows) shows hypoenhancement during the portal phase of CEUS after TACE. (f) Radiofrequency ablation (RFA) is then performed and CEMRI shows non-enhancement (arrows) in the arterial phase 1 month after RFA, indicating a complete response. The LOGIQ E9 scanner was obtained from GE Healthcare, Milwaukee, WI.

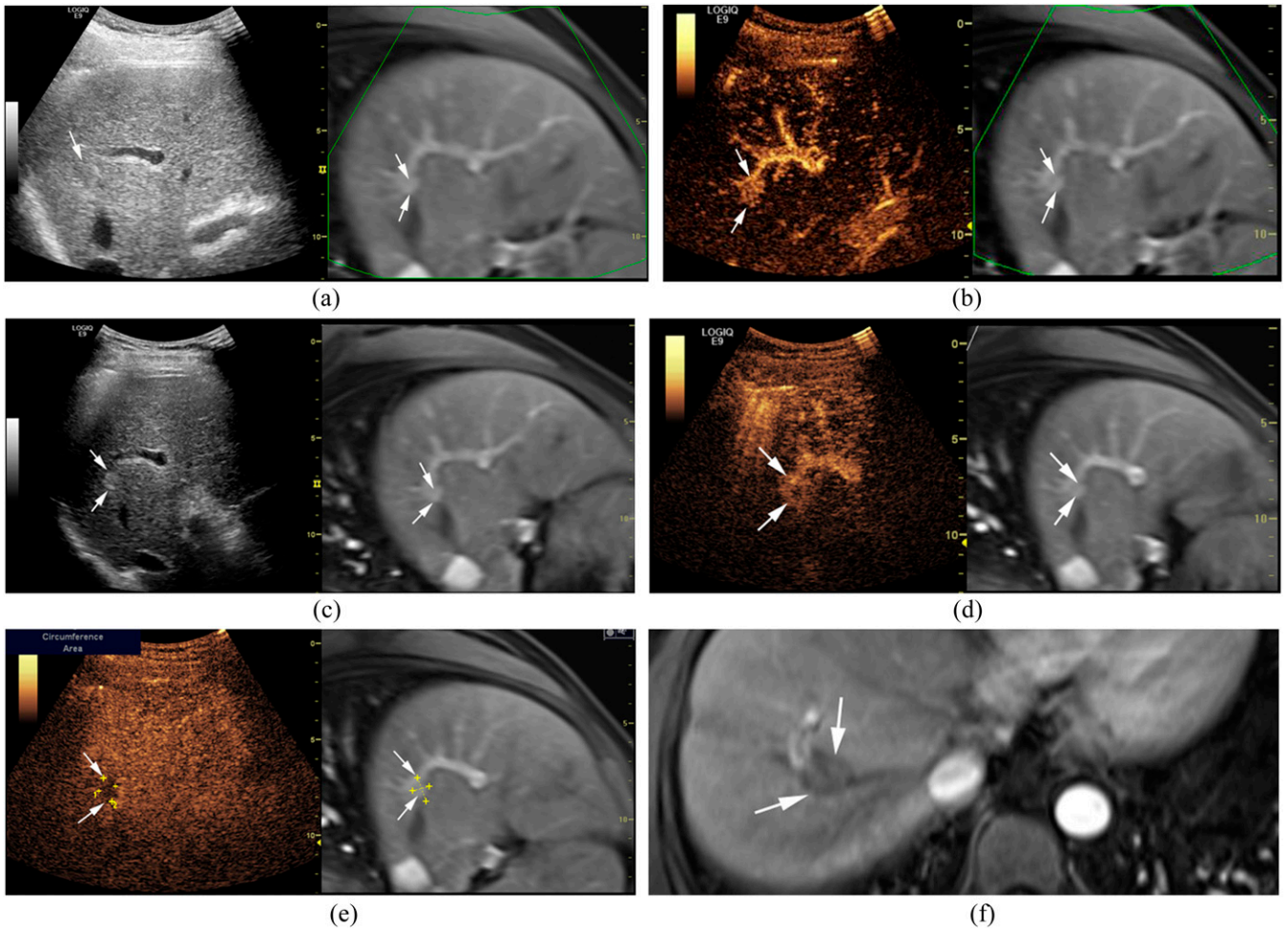

and the conspicuous lesions on conventional ultrasound was performed using Fisher exact test. The confidence level of the operator before and after fusion imaging was compared using the Wilcoxon signed-ranks test. A two-tailed $p < 0.05$ was considered as statistical significance.

RESULTS

Of the 70 lesions, 25 (35.7%, 25/70) could be visualized conspicuously on conventional ultrasound, whereas 45 (64.3%, 45/70) were inconspicuous (Figure 1). There were no significant differences between the inconspicuous and conspicuous lesions on conventional ultrasound with regard to the proportion of the lesions ≤2.0 cm, lesion in the right lobe of the liver, lesion depth ≥5.0 cm, close relationship of the lesion with the capsule and previous treatment history with RFA or TACE (all $p > 0.05$) (Table 2). Inconspicuous lesions on conventional ultrasound were more commonly found in the isoechoic lesions, close relationship of the lesion with the great blood vessels (Figure 1), patients with associated liver background of chronic virus hepatitis, hepatic cirrhosis or severe fatty liver in comparison with the conspicuous lesions (all $p < 0.05$) (Table 2).

Ultrasound-CECT/CEMRI fusion imaging detected additional 24 lesions thus increased the number of the conspicuous lesions to 49 (70.0%) (70.0% *vs* 35.7%; $p < 0.001$ in comparison with conventional ultrasound). CEUS and CECT/CEMRI fusion imaging (Figure 2), however, further increased the number of the conspicuous lesions to 67 (95.7%, 67/70) (95.7% *vs* 70.0%, 95.7% *vs* 35.7%; both $p < 0.001$ in comparison with conventional ultrasound and ultrasound-CECT/CEMRI fusion imaging, respectively), which aided in detecting an additional 18 lesions. In other words, with the assistance of CEUS and CECT/CEMRI fusion imaging, 42(93.3%) of the 45 inconspicuous lesions on conventional ultrasound were detected and located successfully. On the other hand, the confidence level of the operator for performing RFA improved significantly with the use of CEUS and CECT/CEMRI fusion imaging ($p = 0.001$) (Table 3).

Three lesions in two patients were still undetected after using CEUS and CECT/CEMRI fusion imaging. Two lesions were close to the liver capsule and the remaining lesion was near the great blood vessels. These three lesions were subject to radiotherapy and TACE. One lesion close to the gallbladder wall was not appropriate for RFA and was subject to surgery afterwards. Finally, 66 lesions were subject to RFA. The RFA procedures were performed under guidance of conventional ultrasound (54 lesions), ultrasound-CECT/CEMRI fusion imaging (10 lesions) or CEUS and CECT/CEMRI fusion imaging (2 lesions). Technical success of RFA was achieved in 64 lesions with the assistance of fusion imaging system. The CR rate was 97.0% (64/66) in reference to the post-treatment CECT/CEMRI results 1 month after RFA. Two lesions with residual tumours were then subjected to second session of RFA and TACE. No procedure-related death and major complications occurred after RFA. Upper abdomen pain (47.6%, 20/42), slight pleural effusion (26.2%, 11/42) and fever more than 38 °C (9.5%, 4/42) were found several days after RFA and disappeared thereafter. During 3–31 months of follow-up, LTP was found in 8 (12.1%) of 66 lesions and distant recurrence occurred in 14 (33.3%) of 42 patients (13 intrahepatic recurrent lesions and 1 extrahepatic recurrent lesion). The LTP lesions were treated with RFA (five lesions), TACE (one lesion), TACE in combination with RFA (one lesion), percutaneous portal vein perfusion chemotherapy and iodine-125 implantation (one lesion), respectively. The intrahepatic recurrent lesions were treated with RFA (six lesions), TACE (three lesions), TACE in combination with RFA (two lesions), TACE in combination with radiotherapy (one lesion) and iodine-125 implantation (one lesion), respectively. Moreover, one patient with extrahepatic recurrent lesions was treated with radiotherapy and chemotherapy. Two patients died because of liver failure and tumour progression during the follow-up period.

DISCUSSION

Pretreatment clear visualization of the target lesion on ultrasound is a precondition for subsequent ultrasound-guided RFA treatment of liver cancer. However, on conventional ultrasound, many liver cancers are indeterminate or hidden because of interference of bowel gas, lung, bone, limited acoustic window, associated liver cirrhosis or isoechogenicity. These inconspicuous lesions on ultrasound might be detectable on CECT or CEMRI. The concept of fusion imaging of ultrasound and

Table 2. The characteristics for the inconspicuous and conspicuous lesions on conventional ultrasound

Characteristics	Inconspicuous ($n = 45$)	Conspicuous ($n = 25$)	p-value
Lesions ≤2.0 cm	28 (62.2)	11 (44.0)	0.141
Lesions in the right liver lobe	35 (77.8)	18 (72.0)	0.589
Lesion depth ≥5 cm	28 (62.2)	15 (60.0)	0.855
Isoechoic lesions	27 (60.0)	3 (12.0)	<0.001
Lesions close to liver capsule	19 (42.2)	5 (20.0)	0.061
Lesions near to great blood vessels	16 (35.5)	2 (8.0)	0.011
Lesions associated with chronic hepatic disease	28 (62.2)	9 (36.0)	0.035
Lesions treated with RFA or TACE before	6 (13.3)	1 (4.0)	0.408

RFA, radiofrequency ablation; TACE, transcatheter arterial chemoembolization.
Numbers in parentheses are percentages.

Figure 2. A 42-year-old male with a hepatocellular carcinoma lesion (maximum diameter = 2.5 cm) in Segment VIII of the liver and hepatitis B virus-related cirrhosis. (a) The lesion (arrow) is inconspicuous on conventional ultrasound. (b) The lesion (arrows) is inconspicuous on conventional ultrasound even with the assistance of ultrasound-CEMRI fusion imaging. (c) The lesion (arrows) shows hyperenhancement during the arterial phase of contrast-enhanced ultrasound. (d) The size of the ablation zone (arrows) is bigger than that of the previous lesion and RFA electrode needle tract (arrowhead) is displayed in the arterial phase of contrast-enhanced MRI 5 days after RFA. The LOGIQ E9 scanner was obtained from GE Healthcare, Milwaukee, WI.

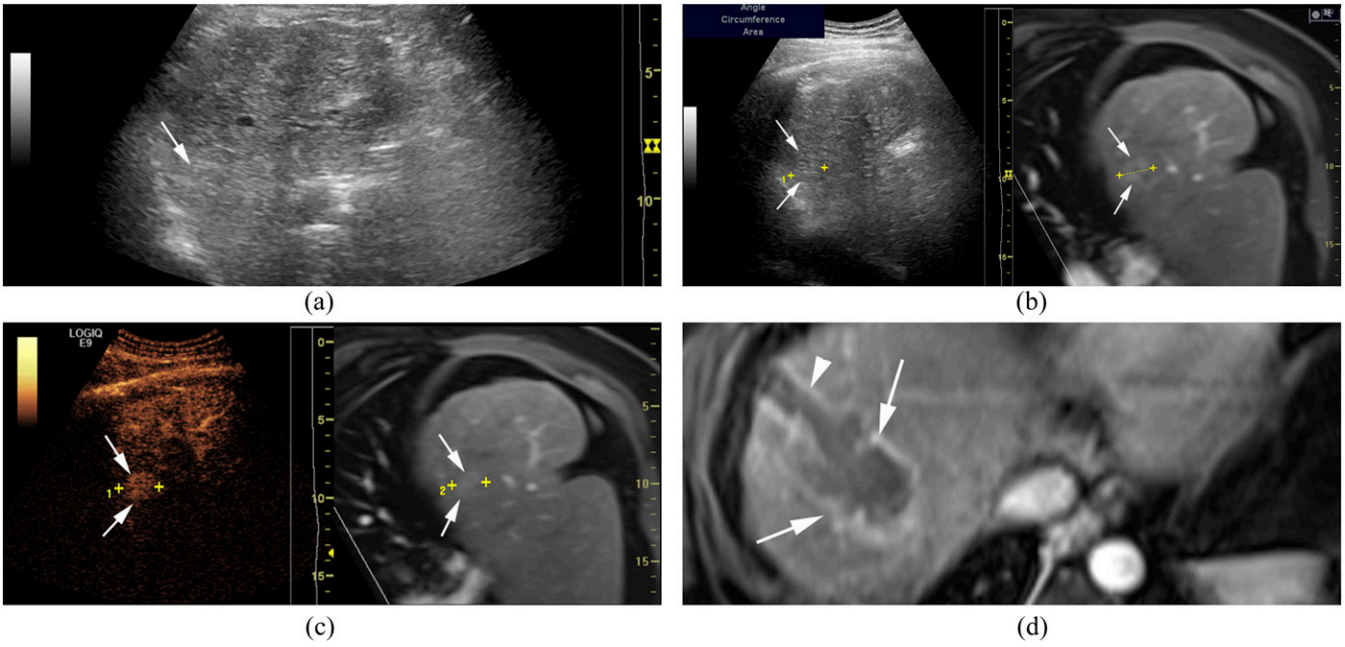

CT/MRI combines the virtues of different imaging modalities, whereas avoids their shortcomings. Thus theoretically, fusion imaging of ultrasound and CT/MRI is helpful to locate and detect those inconspicuous lesions, which would facilitate the following ultrasound-guided interventional procedures.[28–33]

In this series, for those 45 inconspicuous lesions on conventional ultrasound, 53.3% could be detected on ultrasound-CECT/CEMRI fusion imaging, whereas 93.3% lesions could be detected through CEUS and CECT/CEMRI fusion imaging. The number of the conspicuous lesions on conventional ultrasound, ultrasound-CECT/CEMRI fusion imaging and CEUS and CECT/CEMRI fusion imaging accounted for 35.7%, 70.0% and 95.7%, respectively, of the total target lesions. Therefore, CEUS and CECT/CEMRI fusion imaging is more useful than ultrasound-CECT/CEMRI fusion imaging or conventional ultrasound to detect these inconspicuous lesions. Dong et al[25] reported that CEUS-MRI fusion imaging could detect more small HCCs (95.9%, 47/49) than CEUS alone (42.9%, 21/49). Hence, CEUS and CECT/CEMRI fusion imaging is the optimal option for the lesions with poor conspicuity on conventional ultrasound. The convenience, real-time imaging of CEUS and high spatial resolution of CECT/CEMRI is particularly suitable for ultrasound-guided RFA, which can be carried out in the operating room or outpatient unit instead of the CT/MRI room thus greatly reducing occupation of medical resource and possible radiation. Therefore, although CEUS is usually performed in patients with liver lesions who could not receive CT or MRI contrast and ultrasound contrast increases the cost, it is justified for the use of CEUS in the same set of patients. CEUS was successfully carried out in all the patients thus there is no doubt about its feasibility. However, three lesions remained invisible with CEUS and CECT/CEMRI fusion imaging, which may be ascribed to the inspiration and cardiac movement, not-rigid

Table 3. The confidence level of the operator for performing radiofrequency ablation (RFA) on conventional ultrasound and contrast-enhanced ultrasound (CEUS)-contrast-enhanced CT (CECT)/contrast-enhanced MRI (CEMRI) fusion imaging

Levels	Conventional ultrasound ($n = 70$)	CEUS and CECT/CEMRI fusion imaging ($n = 70$)	p-value
I	34 (48.6)	3 (4.3)	0.001
II	11 (15.7)	25 (35.7)	
III	25 (35.7)	42 (60.0)	

Numbers in parentheses are percentages.
Level I = no confidence for performing RFA; Level II = confident for performing RFA; Level III = highly confident for performing RFA.

nature of liver, error registration, inexperience of operators or the different pharmacokinetics of ultrasound contrast agent.

With respect to the factors associated with suboptimal lesion visualization on conventional ultrasound, the present study showed that lesion size, depth, location, previous treatment history with RFA or TACE did not show significant differences between the inconspicuous and the conspicuous lesions on conventional ultrasound. However, Kunishi et al[21] and Lee et al[34] reported that lesions <2 cm were hard to detect, and most of the inconspicuous lesions on conventional ultrasound were actually <2 cm (62.2%, 28/45) in the current study. Previous investigations[29,31] also reported that the deeply located lesions in the liver were difficult to observe on ultrasound images. Lesions with previous RFA or TACE might also affect the lesion conspicuity on conventional ultrasound.[19] The different results might be associated with the limited sample size in this study thus future prospective study with large sample size is mandatory. On the other hand, echogenicity affects lesion conspicuity such that isoechoic lesions were hard to be detected. The study also showed that the lesions close to the great blood vessels were hard to detect, which may be sheltered from the wall of larger blood vessels. Finally, patients with chronic hepatitis, hepatic cirrhosis or severe fatty liver will make liver lesions difficult to detect on conventional ultrasound.[35–38]

In the current study, pre-treatment conventional ultrasound showed that inconspicuous lesions accounted for 64.3% of all the lesions confirmed by CECT/CEMRI, thus conventional ultrasound-guided RFA is not suitable for them. Instead, guidance by other imaging modalities or referral to other treatment methods had to be carried out. However, with the help of CEUS and CECT/CEMRI fusion imaging, 97.0% (64/66) lesions were successfully ablated without any major complications or procedure-related deaths, which showed that CEUS and CECT/CEMRI fusion imaging significantly broadened the indication of ultrasound-guided RFA. It is relevant for those who are not willing to undergo operation or those whose lesions are inoperable. Mauri et al[20] showed that 95.6% (282/295) of tumours were correctly targeted and 90.2% (266/285) of tumours were successfully ablated with no perioperative deaths and 0.9% major complications using real-time ultrasound-CT/MRI guided. Min et al[39] and Minami et al[40] also reported that combination of CEUS and fusion imaging was highly effective in percutaneous RFA for HCC with poor conspicuity on conventional ultrasound.

There are several limitations in our study. First, the selection bias would occur because this was a retrospective single-centre study. The rationale for the study was that all the lesions should be confirmed on CECT/CEMRI before RFA. There might be lesions that were invisible on both ultrasound and CECT/CEMRI, thus further prospective and randomized controlled multicentre studies are warranted to compare the usefulness of CEUS, ultrasound-CECT/CEMRI and CEUS and CECT/CEMRI fusion imaging in detecting liver lesions and guiding RFA. Second, the fusion imaging was operated by one operator, thus the interobserver agreement of this technique was not analyzed. There must be a learning curve for mastering this technique; however, the evaluation was performed by two experienced operators with consensus. Thirdly, the registration error was not analyzed in this study; however, the spatial accuracy of this system had already been verified by some previous studies.[41,42] Finally, the confidence in performing RFA depends on several factors other than the lesion localization. This study mentioned the level of confidence in performing the RFA procedure with the available guidance, which might be subjective. However, the lesion conspicuity is the most significant factor for operators' confidence and the evaluation was based on two experienced operators, thus the influence could be reduced at the largest.

CONCLUSION

Fusion of conventional ultrasound and CECT/CEMRI improves the visualization of inconspicuous liver lesions on conventional ultrasound. This improvement is further enhanced with the utilization of fusion of CEUS and CECT/CEMRI. Fusion of CEUS and CECT/CEMRI also facilitates improvement of the operators' confidence level for performing RFA. Both of them help to achieve CR of RFA.

FUNDING

This work was supported in part by grants 20114003 and 2013SY066 from Shanghai Municipal Commission of Health and Family Planning, grant 14441900900 from Science and Technology Commission of Shanghai Municipality, grants 81301299, 81301229 and 81371570 from the National Natural Scientific Foundation of China and grant SHDC 22015005 from the Shanghai Hospital Development Centre.

REFERENCES

1. Tinkle CL, Haas-Kogan D. Hepatocellular carcinoma: natural history, current management, and emerging tools. *Biologics* 2012; **6**: 207–19. doi: http://dx.doi.org/10.2147/BTT.S23907
2. Liu CY, Chen KF, Chen PJ. Treatment of liver cancer. *Cold Spring Harb Perspect Med* 2015; **5**: a021535. doi: http://dx.doi.org/10.1101/cshperspect.a021535
3. Forner A, Llovet JM, Bruix J. Hepatocellular carcinoma. *Lancet* 2012; **379**: 1245–55. doi: http://dx.doi.org/10.1016/S0140-6736(11)61347-0
4. Cha CH, Saif MW, Yamane BH, Weber SM. Hepatocellular carcinoma: current management. *Curr Probl Surg* 2010; **47**: 10–67. doi: http://dx.doi.org/10.1067/j.cpsurg.2009.09.003
5. Livraghi T, Solbiati L, Meloni MF, Gazelle GS, Halpern EF, Goldberg SN. Treatment of focal liver tumors with percutaneous radio-frequency ablation: complications encountered in a multicenter study. *Radiology* 2003; **226**: 441–51. doi: http://dx.doi.org/10.1148/radiol.2262012198
6. Solbiati L, Ahmed M, Cova L, Ierace T, Brioschi M, Goldberg SN. Small liver colorectal metastases treated with percutaneous radiofrequency ablation: local response rate and long-term survival with up to 10-year follow-up. *Radiology* 2012; **265**: 958–68. doi: http://dx.doi.org/10.1148/radiol.12111851

7. Gillams A, Goldberg N, Ahmed M, Bale R, Breen D, Callstrom M, et al. Thermal ablation of colorectal liver metastases: a position paper by an international panel of ablation experts, The Interventional Oncology Sans Frontieres meeting 2013. *Eur Radiol* 2015; **25**: 3438–54. doi: http://dx.doi.org/10.1007/s00330-015-3779-z
8. Livraghi T, Meloni F, Di Stasi M, Rolle E, Solbiati L, Tinelli C, et al. Sustained complete response and complications rates after radiofrequency ablation of very early hepatocellular carcinoma in cirrhosis: is resection still the treatment of choice? *Hepatology* 2008; **47**: 82–9. doi: http://dx.doi.org/10.1002/hep.21933
9. Wu J, Chen P, Xie YG, Gong NM, Sun LL, Sun CF. Comparison of the effectiveness and safety of ultrasound- and CT-guided percutaneous radiofrequency ablation of non-operation hepatocellular carcinoma. *Pathol Oncol Res* 2015; **21**: 637–42. doi: http://dx.doi.org/10.1007/s12253-014-9868-5
10. Xu HX. Contrast-enhanced ultrasound: the evolving applications. *World J Radiol* 2009; **1**: 15–24. doi: http://dx.doi.org/10.4329/wjr.v1.i1.15
11. Wong GL, Xu HX, Xie XY. Detection of focal liver lesions in cirrhotic liver using contrast-enhanced ultrasound. *World J Radiol* 2009; **1**: 25–36. doi: http://dx.doi.org/10.4329/wjr.v1.i1.25
12. Kang TW, Rhim H. Recent advances in tumor ablation for hepatocellular carcinoma. *Liver Cancer* 2015; **4**: 176–87. doi: http://dx.doi.org/10.1159/000367740
13. Albrecht T, Blomley MJ, Burns PN, Wilson S, Harvey CJ, Leen E, et al. Improved detection of hepatic metastases with pulse-inversion US during the liver-specific phase of SHU 508A: multicenter study. *Radiology* 2003; **227**: 361–70. doi: http://dx.doi.org/10.1148/radiol.2272011833
14. Liu GJ, Xu HX, Lu MD, Xie XY, Xu ZF, Zheng YL, et al. Enhancement pattern of hepatocellular carcinoma: comparison of real-time contrast-enhanced ultrasound and contrast-enhanced computed tomography. *Clin Imaging* 2006; **30**: 315–21. doi: http://dx.doi.org/10.1016/j.clinimag.2006.03.031
15. Westwood M, Joore M, Grutters J, Redekop K, Armstrong N, Lee K, et al. Contrast-enhanced ultrasound using SonoVue® (sulphur hexafluoride microbubbles) compared with contrast-enhanced computed tomography and contrast-enhanced magnetic resonance imaging for the characterisation of focal liver lesions and detection of liver metastases: a systematic review and cost-effectiveness analysis. *Health Technol Assess* 2013; **17**: 1–243. doi: http://dx.doi.org/10.3310/hta17160
16. Xie L, Guang Y, Ding H, Cai A, Huang Y. Diagnostic value of contrast-enhanced ultrasound, computed tomography and magnetic resonance imaging for focal liver lesions: a meta-analysis. *Ultrasound Med Biol* 2011; **37**: 854–61. doi: http://dx.doi.org/10.1016/j.ultrasmedbio.2011.03.006
17. Minami Y, Chung H, Kudo M, Kitai S, Takahashi S, Inoue T, et al. Radiofrequency ablation of hepatocellular carcinoma: value of virtual CT sonography with magnetic navigation. *AJR Am J Roentgenol* 2008; **190**: W335–41. doi: http://dx.doi.org/10.2214/AJR.07.3092
18. Venkatesan AM, Kadoury S, Abi-Jaoudeh N, Levy EB, Maass-Moreno R, Krücker J, et al. Real-time FDG PET guidance during biopsies and radiofrequency ablation using multimodality fusion with electromagnetic navigation. *Radiology* 2011; **260**: 848–56. doi: http://dx.doi.org/10.1148/radiol.11101985
19. Xu HX, Lu MD, Liu LN, Guo LH. Magnetic navigation in ultrasound-guided interventional radiology procedures. *Clin Radiol* 2012; **67**: 447–54. doi: http://dx.doi.org/10.1016/j.crad.2011.10.015
20. Mauri G, Cova L, De Beni S, Ierace T, Tondolo T, Cerri A, et al. Real-time US-CT/MRI image fusion for guidance of thermal ablation of liver tumors undetectable with US: results in 295 cases. *Cardiovasc Intervent Radiol* 2015; **38**: 143–51. doi: http://dx.doi.org/10.1007/s00270-014-0897-y
21. Kunishi Y, Numata K, Morimoto M, Okada M, Kaneko T, Maeda S, et al. Efficacy of fusion imaging combining sonography and hepatobiliary phase MRI with Gd-EOB-DTPA to detect small hepatocellular carcinoma. *AJR Am J Roentgenol* 2012; **198**: 106–14. doi: http://dx.doi.org/10.2214/AJR.10.6039
22. Song KD, Lee MW, Rhim H, Cha DI, Chong Y, Lim HK. Fusion imaging-guided radiofrequency ablation for hepatocellular carcinomas not visible on conventional ultrasound. *AJR Am J Roentgenol* 2013; **201**: 1141–7. doi: http://dx.doi.org/10.2214/AJR.13.10532
23. Diana M, Halvax P, Mertz D, Legner A, Brulé JM, Robinet E, et al. Improving echo-guided procedures using an ultrasound-CT image fusion system. *Surg Innov* 2015; **22**: 217–22. doi: http://dx.doi.org/10.1177/1553350615577483
24. Maeda T, Hong J, Konishi K, Nakatsuji T, Yasunaga T, Yamashita Y, et al. Tumor ablation therapy of liver cancers with an open magnetic resonance imaging-based navigation system. *Surg Endosc* 2009; **23**: 1048–53. doi: http://dx.doi.org/10.1007/s00464-008-0123-6
25. Lee JY, Choi BI, Chung YE, Kim MW, Kim SH, Han JK. Clinical value of CT/MR-US fusion imaging for radiofrequency ablation of hepatic nodules. *Eur J Radiol* 2012; **81**: 2281–9. doi: http://dx.doi.org/10.1016/j.ejrad.2011.08.013
26. Lee MW, Rhim H, Cha DI, Kim YJ, Choi D, Kim YS, et al. Percutaneous radiofrequency ablation of hepatocellular carcinoma: fusion imaging guidance for management of lesions with poor conspicuity at conventional sonography. *AJR Am J Roentgenol* 2012; **198**: 1438–44. doi: http://dx.doi.org/10.2214/AJR.11.7568
27. Bruix J, Sherman M; American Association for the Study of Liver Diseases. Management of hepatocellular carcinoma: an update. *Hepatology* 2011; **53**: 1020–2. doi: http://dx.doi.org/10.1002/hep.24199
28. Jung EM, Friedrich C, Hoffstetter P, Dendl LM, Klebl F, Agha A, et al. Volume navigation with contrast enhanced ultrasound and image fusion for percutaneous interventions: first results. *PLoS One* 2012; **7**: e33956. doi: http://dx.doi.org/10.1371/journal.pone.0033956
29. Dong Y, Wang WP, Mao F, Ji ZB, Huang BJ. Application of imaging fusion combining contrast-enhanced ultrasound and magnetic resonance imaging in detection of hepatic cellular carcinomas undetectable by conventional ultrasound. *J Gastroenterol Hepatol* 2016; **31**: 822–8. doi: http://dx.doi.org/10.1111/jgh.13202
30. Meijerink MR, van Waesberghe JH, van der Weide L, van den Tol P, Meijer S, van Kuijk C. Total-liver-volume perfusion CT using 3-D image fusion to improve detection and characterization of liver metastases. *Eur Radiol* 2008; **18**: 2345–54. doi: http://dx.doi.org/10.1007/s00330-008-0996-8
31. Liu FY, Yu XL, Liang P, Cheng ZG, Han ZY, Dong BW, et al. Microwave ablation assisted by a real-time virtual navigation system for hepatocellular carcinoma undetectable by conventional ultrasonography. *Eur J Radiol* 2012; **81**: 1455–9. doi: http://dx.doi.org/10.1016/j.ejrad.2011.03.057
32. Makino Y, Imai Y, Igura T, Kogita S, Sawai Y, Fukuda K, et al. Usefulness of the extracted-overlay function in CT/MR-ultrasonography fusion imaging for radiofrequency ablation of hepatocellular carcinoma. *Dig Dis* 2013; **31**: 485–9. doi: http://dx.doi.org/10.1159/000355257
33. Xu ZF, Xie XY, Kuang M, Liu GJ, Chen LD, Zheng YL, et al. Percutaneous radiofrequency ablation of malignant liver tumors with ultrasound and CT fusion imaging guidance. *J Clin Ultrasound* 2014; **42**: 321–30. doi: http://dx.doi.org/10.1002/jcu.22141

34. Lee MW, Rhim H, Cha DI, Kim YJ, Lim HK. Planning US for percutaneous radiofrequency ablation of small hepatocellular carcinomas (1–3 cm): value of fusion imaging with conventional US and CT/MR images. *J Vasc Interv Radiol* 2013; **24**: 958–65. doi: http://dx.doi.org/10.1016/j.jvir.2013.04.007
35. Numata K, Tanaka K, Kiba T, Matsumoto S, Iwase S, Hara K, et al. Nonresectable hepatocellular carcinoma: improved percutaneous ethanol injection therapy guided by CO(2)-enhanced sonography. *AJR Am J Roentgenol* 2001; **177**: 789–98. doi: http://dx.doi.org/10.2214/ajr.177.4.1770789
36. Numata K, Isozaki T, Ozawa Y, Sakaguchi T, Kiba T, Kubota T, et al. Percutaneous ablation therapy guided by contrast-enhanced sonography for patients with hepatocellular carcinoma. *AJR Am J Roentgenol* 2003; **180**: 143–9. doi: http://dx.doi.org/10.2214/ajr.180.1.1800143
37. Claudon M, Dietrich CF, Choi BI, Cosgrove DO, Kudo M, Nolsøe CP, et al. Guidelines and good clinical practice recommendations for contrast enhanced ultrasound (CEUS) in the liver—update 2012: a WFUMB-EFSUMB initiative in cooperation with representatives of AFSUMB, AIUM, ASUM, FLAUS and ICUS. *Ultraschall Med* 2013; **34**: 11–29. doi: http://dx.doi.org/10.1055/s-0032-1325499
38. Ichikawa T, Saito K, Yoshioka N, Tanimoto A, Gokan T, Takehara Y, et al. Detection and characterization of focal liver lesions: a Japanese phase III, multicenter comparison between gadoxetic acid disodium-enhanced magnetic resonance imaging and contrast-enhanced computed tomography predominantly in patients with hepatocellular carcinoma and chronic liver disease. *Invest Radiol* 2010; **45**: 133–41. doi: http://dx.doi.org/10.1097/RLI.0b013e3181caea5b
39. Min JH, Lim HK, Lim S, Kang TW, Song KD, Choi SY, et al. Radiofrequency ablation of very-early-stage hepatocellular carcinoma inconspicuous on fusion imaging with B-mode US: value of fusion imaging with contrast-enhanced US. *Clin Mol Hepatol* 2014; **20**: 61–70. doi: http://dx.doi.org/10.3350/cmh.2014.20.1.61
40. Minami T, Minami Y, Chishina H, Arizumi T, Takita M, Kitai S, et al. Combination guidance of contrast-enhanced US and fusion imaging in radiofrequency ablation for hepatocellular carcinoma with poor conspicuity on contrast-enhanced US/fusion imaging. *Oncology* 2014; **87**(Suppl. 1): 55–62. doi: http://dx.doi.org/10.1159/000368146
41. Hakime A, Deschamps F, De Carvalho EG, Teriitehau C, Auperin A, De Baere T. Clinical evaluation of spatial accuracy of a fusion imaging technique combining previously acquired computed tomography and real-time ultrasound for imaging of liver metastases. *Cardiovasc Intervent Radiol* 2011; **34**: 338–44. doi: http://dx.doi.org/10.1007/s00270-010-9979-7
42. Krücker J, Xu S, Venkatesan A, Locklin JK, Amalou H, Glossop N, et al. Clinical utility of real-time fusion guidance for biopsy and ablation. *J Vasc Interv Radiol* 2011; **22**: 515–24. doi: http://dx.doi.org/10.1016/j.jvir.2010.10.033